YMTHE, Volume *31*

Supplemental Information

Atractylodinol prevents pulmonary fibrosis through inhibiting TGF-β receptor 1 recycling by stabilizing vimentin

Mengjiao Hao, Zhuoji Guan, Zhikang Zhang, Haopeng Ai, Xing Peng, Huihao Zhou, Jun Xu, and Qiong Gu

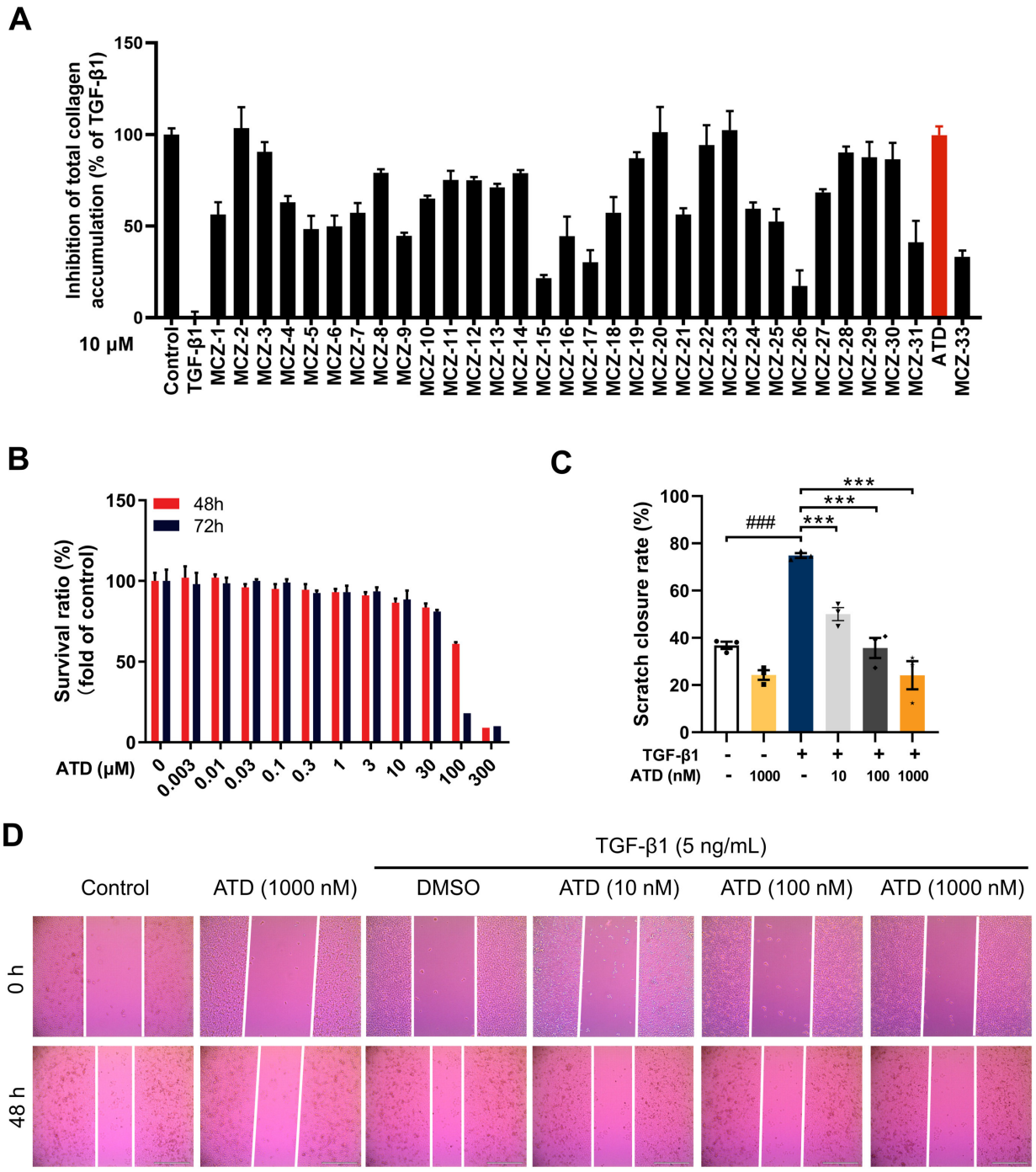

Figure S1. Screening to identify ATD with anti-PF.

(A) Picrosirius red staining of HFL1 cells showed collagen accumulation after treated with 10 μM compounds. Triplicates were performed. (B) Relative viability measurements of the HFL1 cells after 48 hours or 72 hours treatment with ATD (n = 3). (C) Quantification of scratch closure rate (n = 3). (D) Scratch recorded after exposing to ATD in A549 cell wound healing assay. Scale bar: 400 μm. The data are presented as the mean ± SEM. $^{\#}P < 0.05$, $^{\#\#}P < 0.01$, $^{\#\#\#}P < 0.001$ compared

to control group; * $P < 0.05$, ** $P < 0.01$, *** $P < 0.001$ compared to TGF-β1 group. ns: no statistical difference.

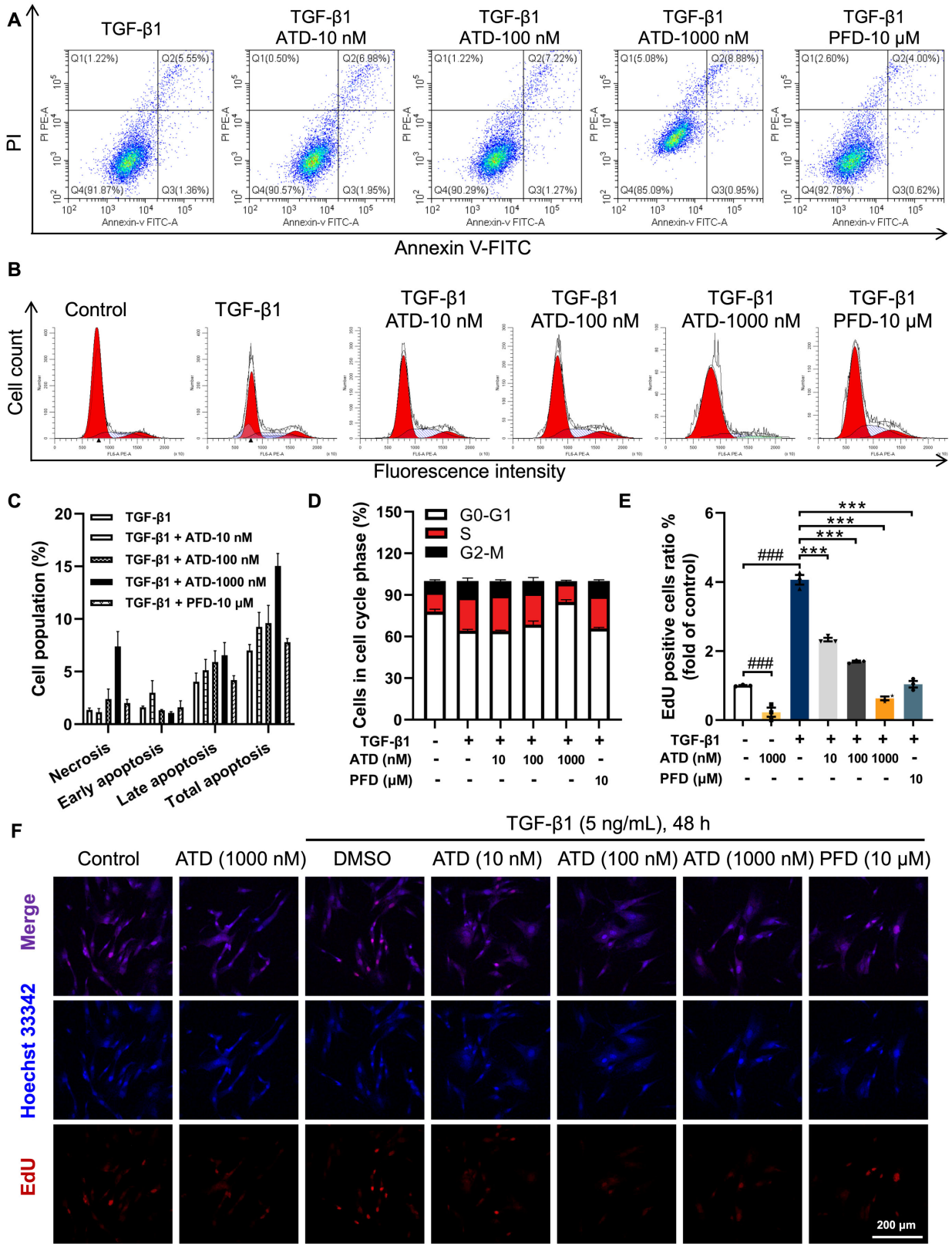
A
TGF-β1
TGF-β1 ATD-10 nM
TGF-β1 ATD-100 nM
TGF-β1 ATD-1000 nM
TGF-β1 PFD-10 μM
PI
Annexin V-FITC
Q1(1.22%)
Q2(5.55%)
Q4(91.87%)
Q3(1.36%)
Q1(0.50%)
Q2(6.98%)
Q4(90.57%)
Q3(1.95%)
Q1(1.22%)
Q2(7.22%)
Q4(90.29%)
Q3(1.27%)
Q1(5.08%)
Q2(8.88%)
Q4(85.09%)
Q3(0.95%)
Q1(2.60%)
Q2(4.00%)
Q4(92.78%)
Q3(0.62%)
B
Control
TGF-β1
TGF-β1 ATD-10 nM
TGF-β1 ATD-100 nM
TGF-β1 ATD-1000 nM
TGF-β1 PFD-10 μM
Cell count
Fluorescence intensity
C
Cell population (%)
TGF-β1
TGF-β1 + ATD-10 nM
TGF-β1 + ATD-100 nM
TGF-β1 + ATD-1000 nM
TGF-β1 + PFD-10 μM
Necrosis
Early apoptosis
Late apoptosis
Total apoptosis
D
Cells in cell cycle phase (%)
G0-G1
S
G2-M
TGF-β1
ATD (nM)
PFD (μM)
E
EdU positive cells ratio % (fold of control)
###
***
TGF-β1
ATD (nM)
PFD (μM)
F
TGF-β1 (5 ng/mL), 48 h
Control
ATD (1000 nM)
DMSO
ATD (10 nM)
ATD (100 nM)
ATD (1000 nM)
PFD (10 μM)
Merge
Hoechst 33342
EdU
200 μm

Figure S2. ATD promotes apoptosis and inhibits excessive proliferation of HFL1 cells.

(A) HFL1 cells were treated with different concentrations of ATD for 48 hours, and then the apoptotic cells were assessed by Annexin VAlexa Fluor 488/PI apoptosis detection kit. (B) HFL1 cells were treated with different concentrations of ATD for 48 hours, and then the cells cycle were assessed by PI staining. (C) The percentage of apoptotic HFL1 cells was measured with flow cytometry (n = 3). (D) The distribution of HFL1 cells (%) treated with ATD in each cell-cycle phase (n = 3). (E) The EdU positive cells ratio of the HFL1 cells after 48 hours treatment with ATD (n = 3). (F) The HFL1 cells were incubated with different concentrations of ATD in the presence or absence of TGF-β1 stimulation for 48 hours, and were detected by the EdU staining kit. Scale bar: 200 μm. The data are presented as the mean ± SEM. $^{\#}$ $P < 0.05$, $^{\#\#}$ $P < 0.01$, $^{\#\#\#}$ $P < 0.001$ compared to control group; * $P < 0.05$, ** $P < 0.01$, *** $P < 0.001$ compared to TGF-β1 group. ns: no statistical difference.

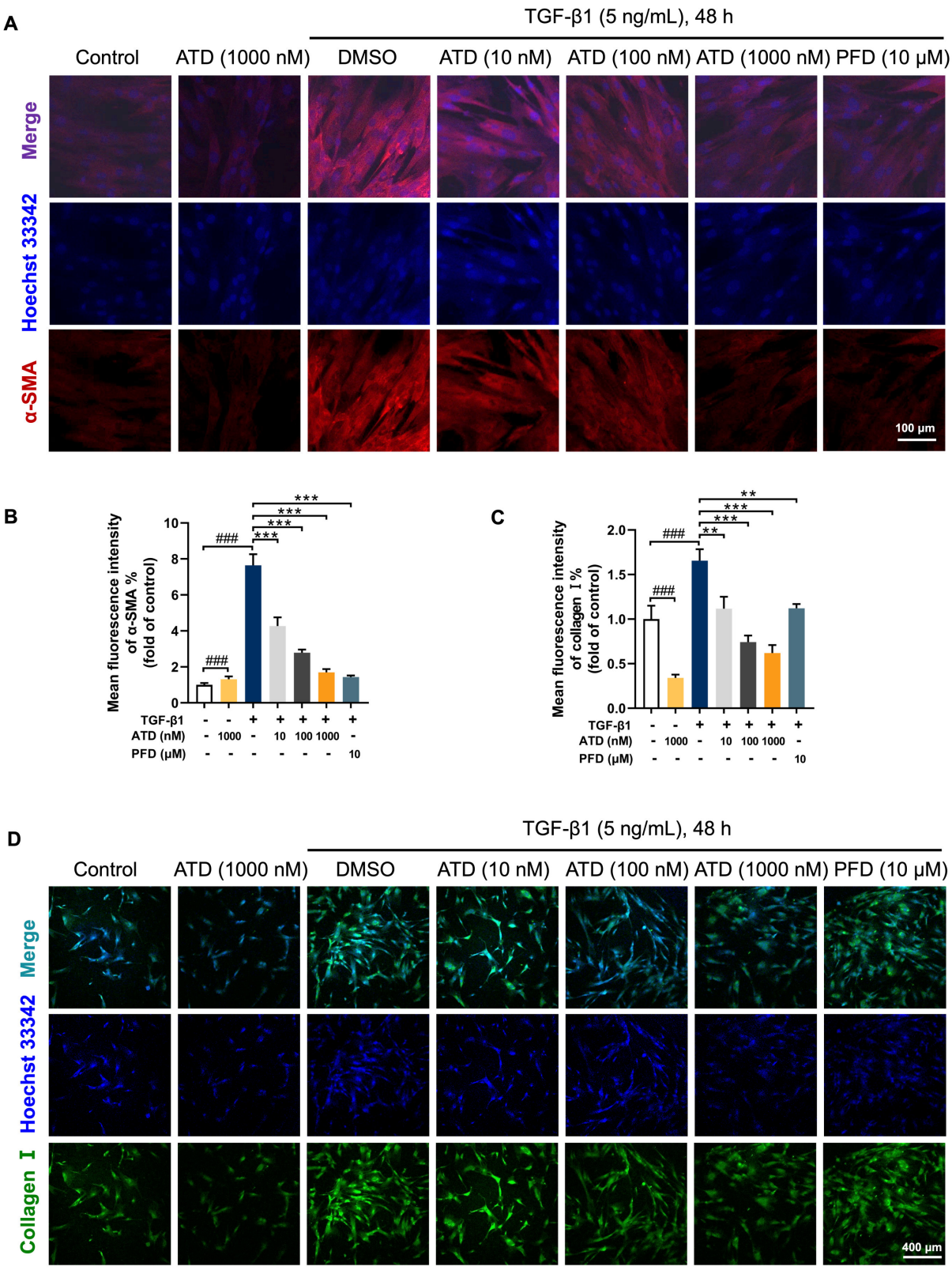
A
TGF-β1 (5 ng/mL), 48 h
Control
ATD (1000 nM)
DMSO
ATD (10 nM)
ATD (100 nM)
ATD (1000 nM)
PFD (10 μM)
Merge
Hoechst 33342
α-SMA
100 μm
B
Mean fluorescence intensity of α-SMA % (fold of control)
TGF-β1
ATD (nM)
PFD (μM)
C
Mean fluorescence intensity of collagen I % (fold of control)
D
Collagen I
400 μm

Figure S3. ATD inhibits the expression of a-SMA and collagen I in HFL1 cells to improve PF.

(A) The HFL1 cells were incubated with different concentrations of ATD in the presence or absence of TGF-β1 stimulation for 48 hours. The expression of α-SMA was observed by immunofluorescence microscopy. Scale bar: 100 μm. (B) Quantification of the fluorescence intensity of α-SMA ($n = 3$). (C) The expression of collagen I was observed by immunofluorescence microscopy. Scale bar: 400 μm. (D) Quantification of the fluorescence intensity of collagen I ($n = 3$). The data are presented as the mean ± SEM. $^{\#}$ $P < 0.05$, $^{\#\#}$ $P < 0.01$, $^{\#\#\#}$ $P < 0.001$ compared to control group; * $P < 0.05$, ** $P < 0.01$, *** $P < 0.001$ compared to TGF-β1 group.

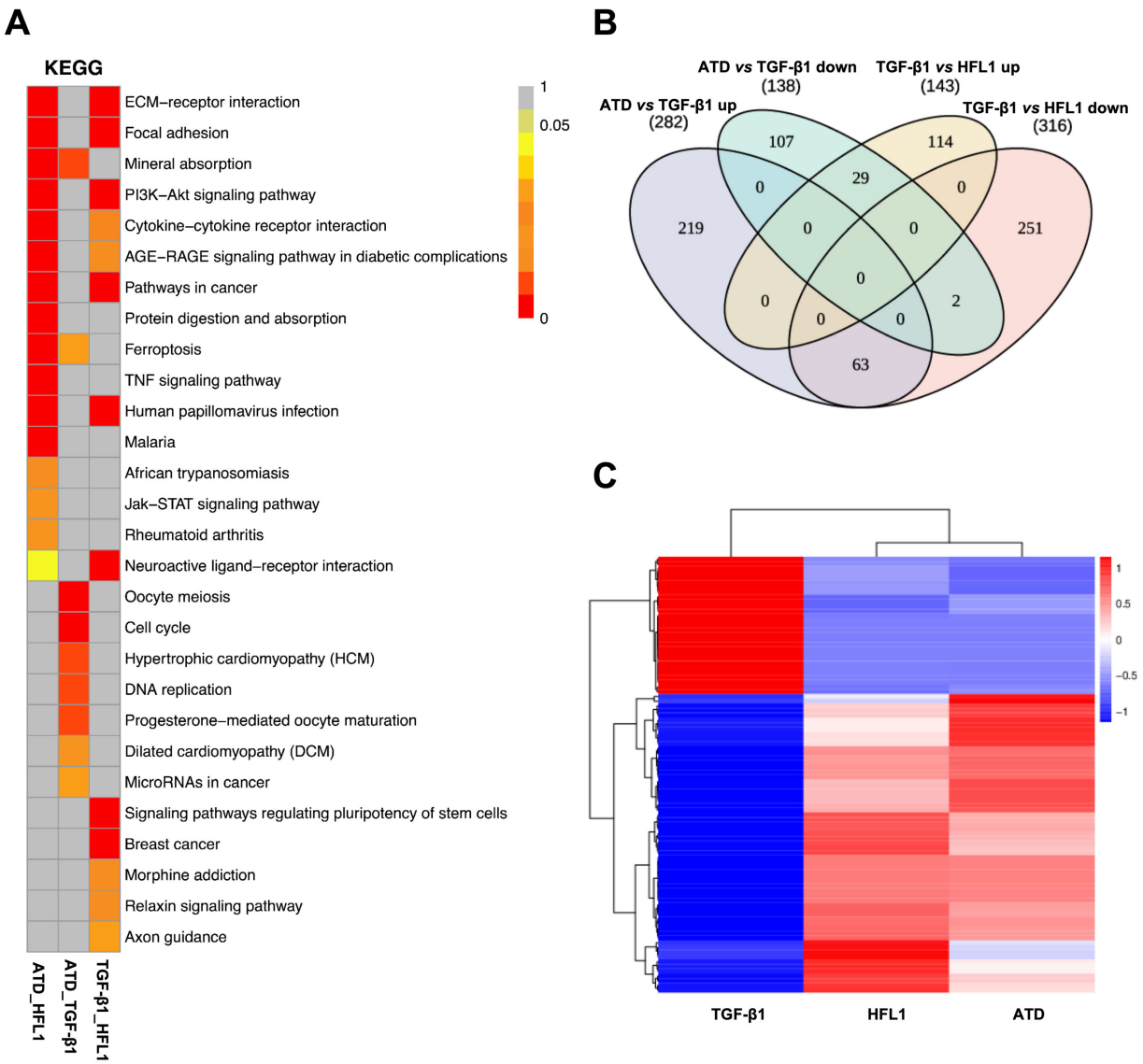

Figure S4. The differentially expressed genes among HFL1 group (Control), TGF-β1 group, and ATD group.

(A) Extract the union of the KEGG enrichment pathway analysis of all comparison groups, and make a distribution map according to the enrichment degree q value of the sample in this pathway. (B) Venn diagram shows the overlap among HFL1, TGF-β1, and ATD group-associated genes. (C) Heatmap illustrating the expression of genes in HFL1, TGF-β1, and ATD group.

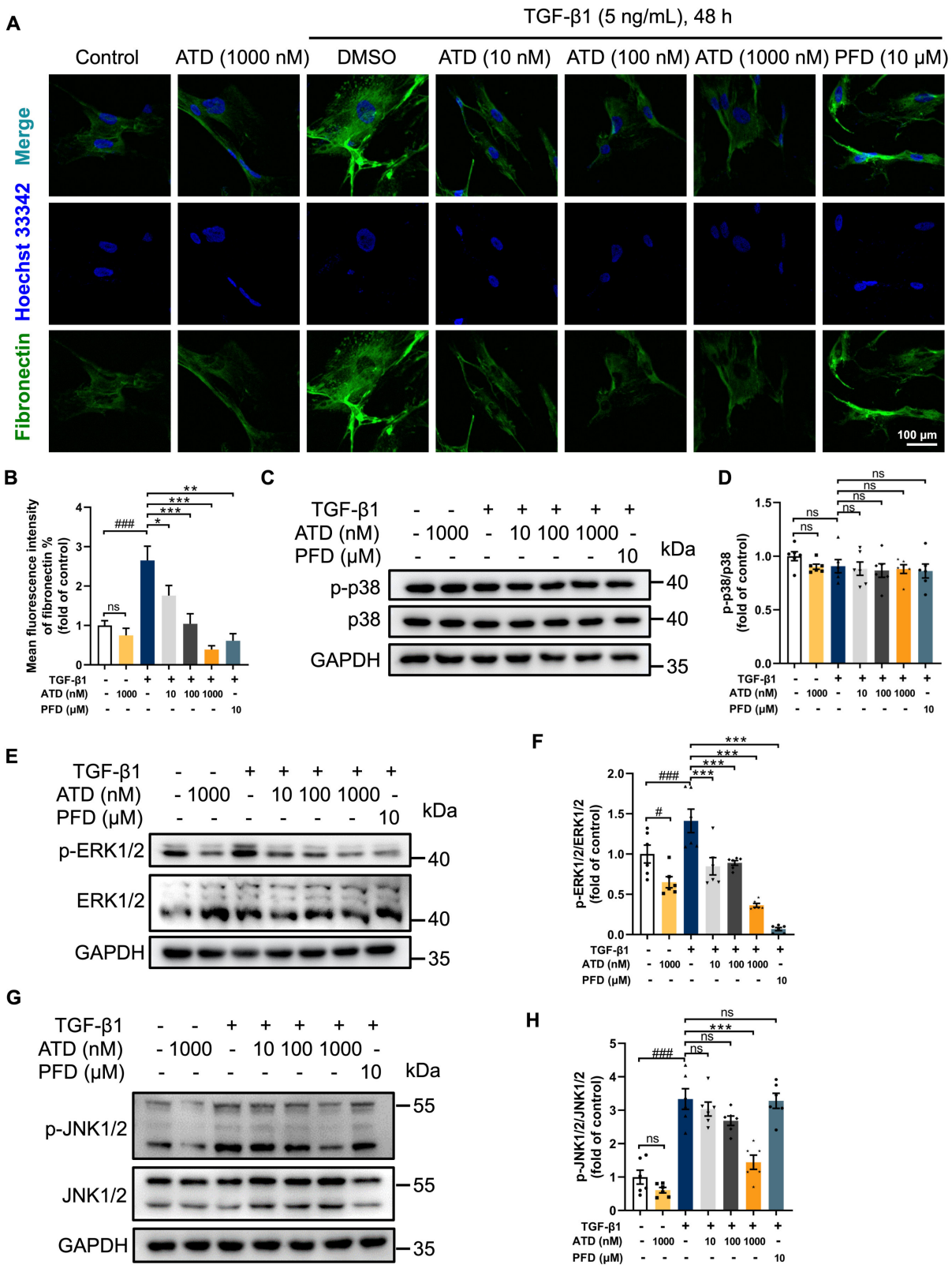
A
TGF-β1 (5 ng/mL), 48 h
Control
ATD (1000 nM)
DMSO
ATD (10 nM)
ATD (100 nM)
ATD (1000 nM)
PFD (10 μM)
Merge
Hoechst 33342
Fibronectin
100 μm
B
Mean fluorescence intensity of fibronectin % (fold of control)
C
TGF-β1
ATD (nM)
PFD (μM)
kDa
p-p38
p38
GAPDH
D
p-p38/p38 (fold of control)
E
p-ERK1/2
ERK1/2
GAPDH
F
p-ERK1/2/ERK1/2 (fold of control)
G
p-JNK1/2
JNK1/2
GAPDH
H
p-JNK1/2/JNK1/2 (fold of control)

Figure S5. ATD prevents PF *via* inhibition ERK1/2 and JNK1/2 phosphorylation.

(A) The expression of fibronectin was observed by immunofluorescence microscopy. Scale bar: 100 μm. (B) Quantification of the fluorescence intensity of fibronectin (n = 3). (C) The protein expression of p-p38 and p38 was analyzed by Western blotting analysis. (D) Quantification of the phosphorylation level of p-p38/p38. (n = 6). (E) The protein expression of p-ERK1/2 and ERK1/2 was analyzed by Western blotting analysis. (F) Quantification of the phosphorylation level of p-ERK1/2 / ERK1/2. (n = 6). (G) The protein expression of p-JNK1/2 and JNK1/2 was analyzed by Western blotting analysis. (H) Quantification of the phosphorylation level of p-JNK1/2 / JNK1/2. (n = 6). The data are presented as the mean ± SEM. $^{\#}P < 0.05$, $^{\#\#}P < 0.01$, $^{\#\#\#}P < 0.001$ compared to control group; * $P < 0.05$, ** $P < 0.01$, *** $P < 0.001$ compared to TGF-β1 group. ns: no statistical difference.

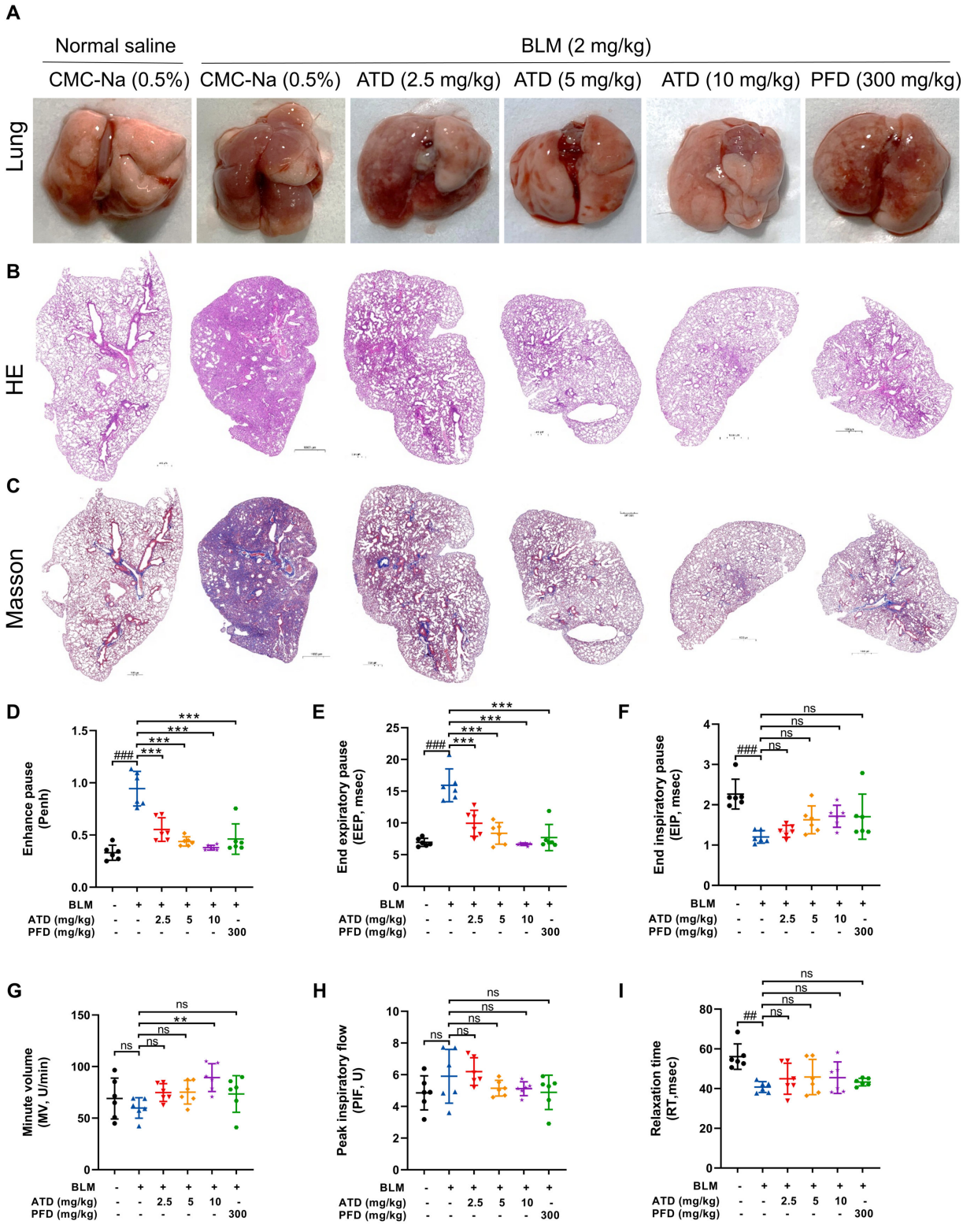
A
Normal saline
BLM (2 mg/kg)
CMC-Na (0.5%)
CMC-Na (0.5%)
ATD (2.5 mg/kg)
ATD (5 mg/kg)
ATD (10 mg/kg)
PFD (300 mg/kg)
Lung
B
HE
C
Masson
D
Enhance pause (Penh)
E
End expiratory pause (EEP, msec)
F
End inspiratory pause (EIP, msec)
G
Minute volume (MV, U/min)
H
Peak inspiratory flow (PIF, U)
I
Relaxation time (RT,msec)
BLM
ATD (mg/kg)
PFD (mg/kg)

Figure S6. ATD protected against PF induced by bleomycin (BLM) in C57BL/6 mice.

(A) Representative images of lung tissue. (B) Representative images of HE staining. (C) Representative images of Masson staining. Representative pulmonary function parameters: (D) enhance pause (Penh), (E) end expiratory pause dynamic (EEP), (F) end inspiratory pause (EIP), (G) minute volume (MV), (H) peak inspiratory flow (PIF) and (I) relaxation time (RT) (n = 6). The data are presented as the mean ± SEM. $^{\#}$ $P < 0.05$, $^{\#\#}$ $P < 0.01$, $^{\#\#\#}$ $P < 0.001$ compared to control group; * $P < 0.05$, ** $P < 0.01$, *** $P < 0.001$ compared to bleomycin group. ns: no statistical difference.

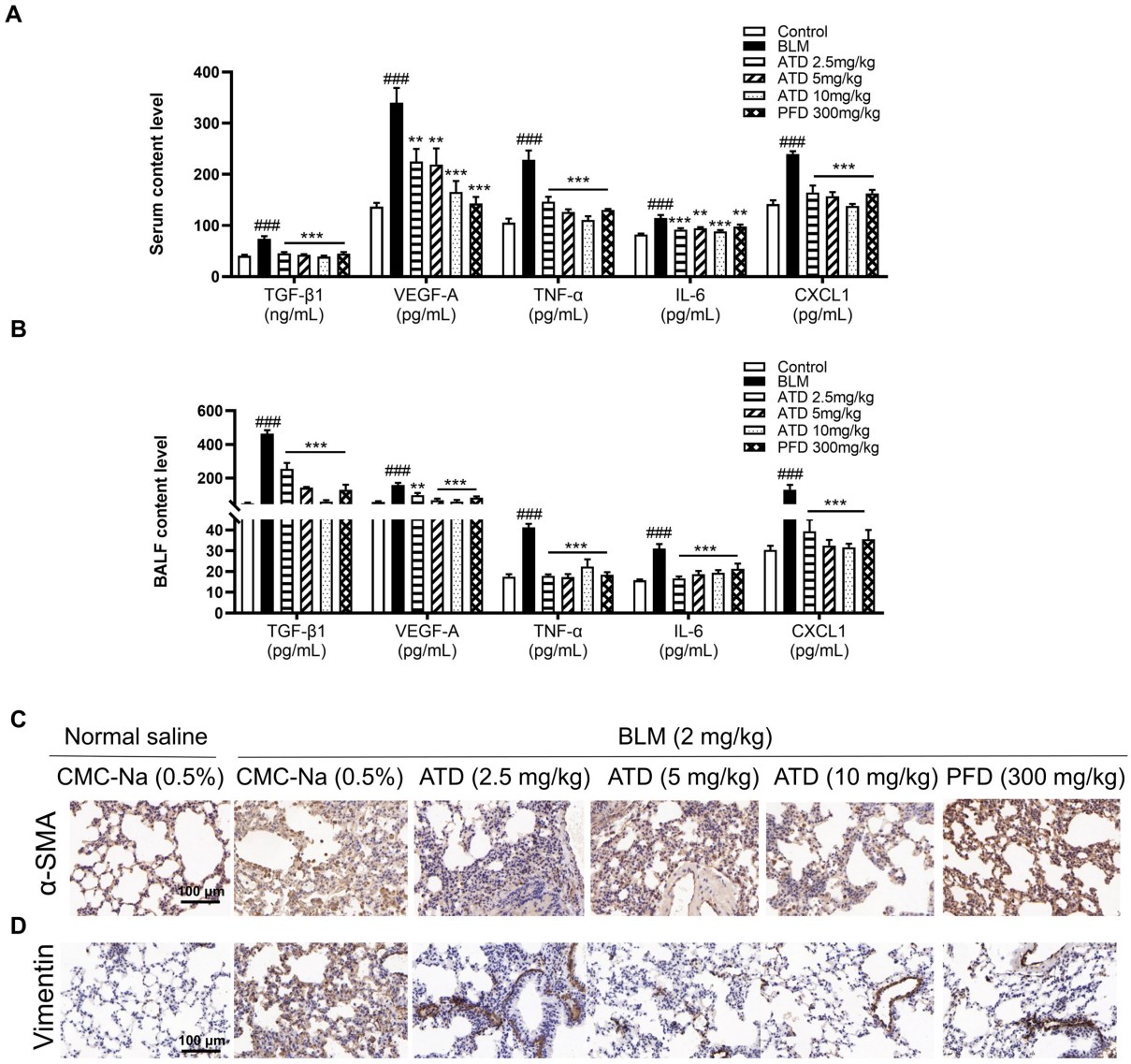

Figure S7. ATD alleviates inflammation and fibrosis induced by bleomycin in C57BL/6 mice.

(A) Secretion levels of transforming growth factor β1 (TGF-β1), vascular endothelial growth factor A (VEGF-A), tumor necrosis factor α (TNF-α), interleukin 6 (IL-6), and chemokine (CXCL1) in serum quantified by enzyme-linked immunosorbent assay (ELISA) kits (n = 6). (B) Secretion levels of TGF-β1, VEGF-A, TNF-α, IL-6, and CXCL1 in bronchoalveolar lavage fluid (BALF) quantified by ELISA kits (n = 6). Representative immunohistochemistry images of (C) α-SMA and (D) vimentin in lung tissue. Scale bar: 100 μm. The data are presented as the mean ± SEM. * $P < 0.05$, ** $P < 0.01$, *** $P < 0.001$ compared to bleomycin group; $^{\#}$ $P < 0.05$, $^{\#\#}$ $P < 0.01$, $^{\#\#\#}$ $P < 0.001$ compared to control. ns: no statistical difference.

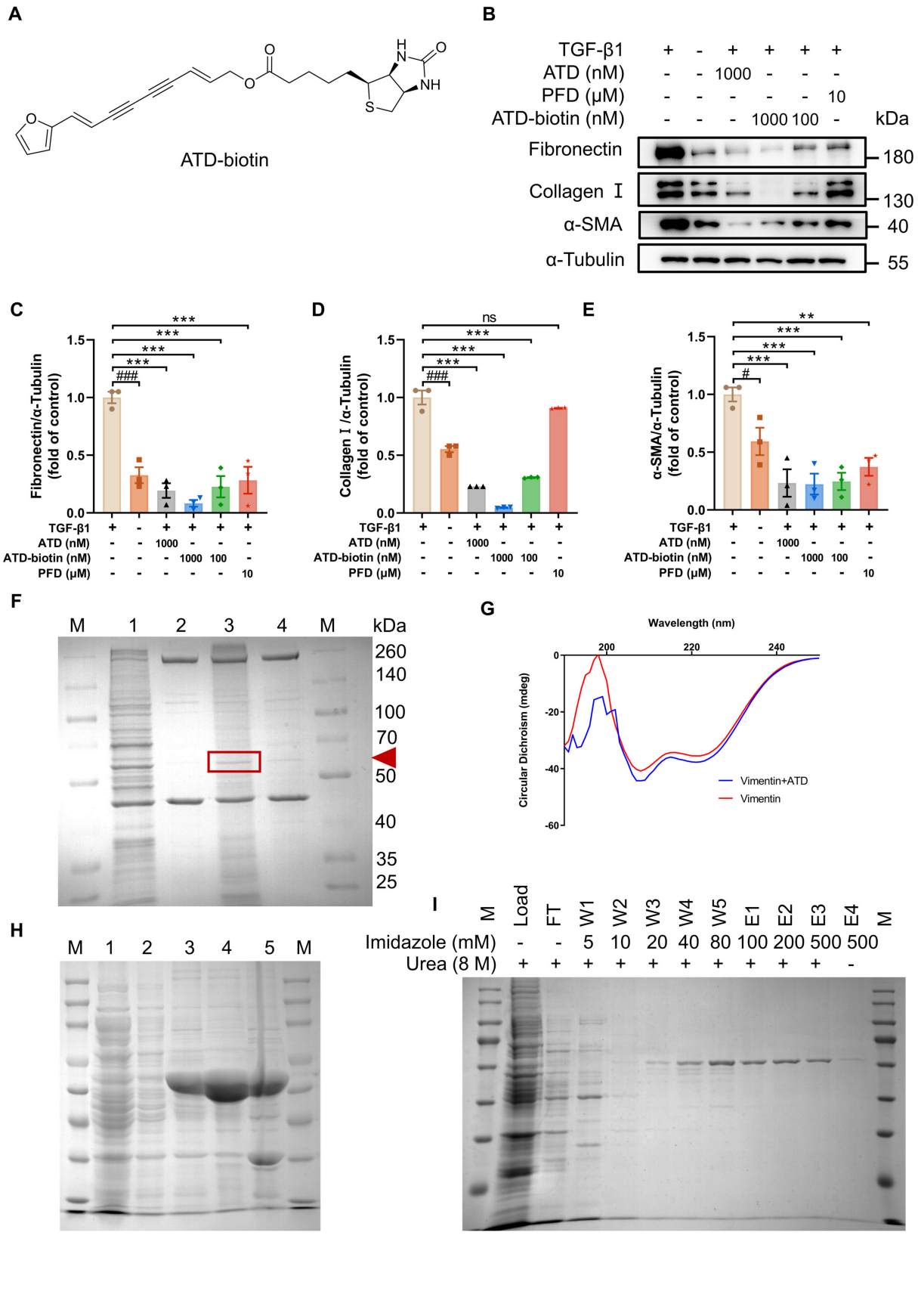
A
ATD-biotin
B
TGF-β1
ATD (nM)
PFD (μM)
ATD-biotin (nM)
kDa
Fibronectin
Collagen Ⅰ
α-SMA
α-Tubulin
180
130
40
55
C
Fibronectin/α-Tubulin (fold of control)
D
Collagen Ⅰ /α-Tubulin (fold of control)
ns
E
α-SMA/α-Tubulin (fold of control)
F
M
kDa
260
140
100
70
50
40
35
25
G
Wavelength (nm)
Circular Dichroism (mdeg)
Vimentin+ATD
Vimentin
H
I
Load
FT
W1
W2
W3
W4
W5
E1
E2
E3
E4
Imidazole (mM)
Urea (8 M)

Figure S8. Target identification of ATD.

(A) Structure of atractylodinol-biotin (ATD-biotin). (B) The protein expression of fibronectin, collagen I, and α-SMA in HFL1 cells was examined by Western blotting analysis (n = 3). Quantification of the protein expression of (C) fibronectin, (D) collagen I and (E) α-SMA. (F) TGF-β1-induced HFL1 cell lysates (lane 1), were incubated overnight at 4 °C with biotin (20 μM, lane 2), ATD-biotin (20 μM, lane 3), or ATD-biotin (10 μM, lane 4). Streptavidin agarose beads were used to capture ATD-biotin-protein complexes. Proteins were run on tris-glycine gel and visualized using coomassie blue stain. (G) CD spectra of VIM (5 μM) and the mixture of VIM and ATD (5 μM). (H) Protein expression and purification. soluble fraction after cell disruption (lane 1); soluble fraction after repeated disruption (lane 2); soluble fraction after treatment with 2 M urea (lane 3); soluble fraction after treatment with 8 M urea (lane 4); insoluble fraction after treatment with 8 M urea (lane 5); M: Molecular weight marker. (I) FT: flow-through; 100 mM to 500 mM imidazole elution fraction is purified vimentin. The data are presented as the mean ± SEM. $^{\#}P < 0.05$, $^{\#\#}P < 0.01$, $^{\#\#\#}P < 0.001$ compared to control group; * $P < 0.05$, ** $P < 0.01$, *** $P < 0.001$ compared to TGF-β1 group. ns: no statistical difference.

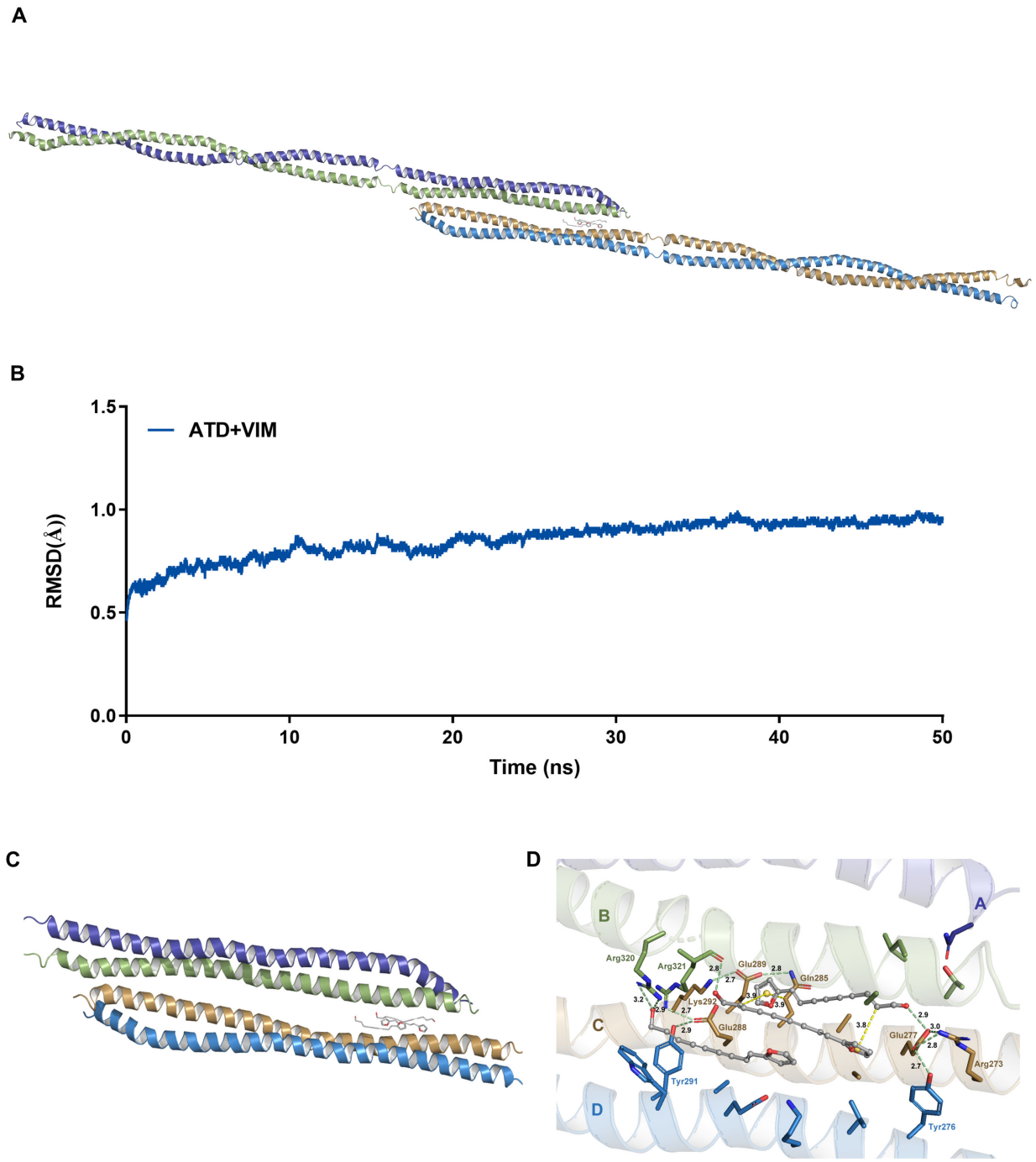

Figure S9. Molecular model of ATD binding site in tetrameric VIM.

(A) A snapshot of the MD-simulated solvent-accessible surface area binding structure showing ATD binding in the cleft between the B and C α helices of the VIM tetramer. (B) Time-series of RMSD of backbone atoms from the starting structures for the complexes over 50 ns of MD simulations. The equilibration phase is not included. (C) A snapshot of the MD-simulated solvent-accessible surface area binding structure showing ATD binding in the cleft between the

B and C α helices of the VIM tetramer. (D) This model shows the interaction between VIM and ATD.

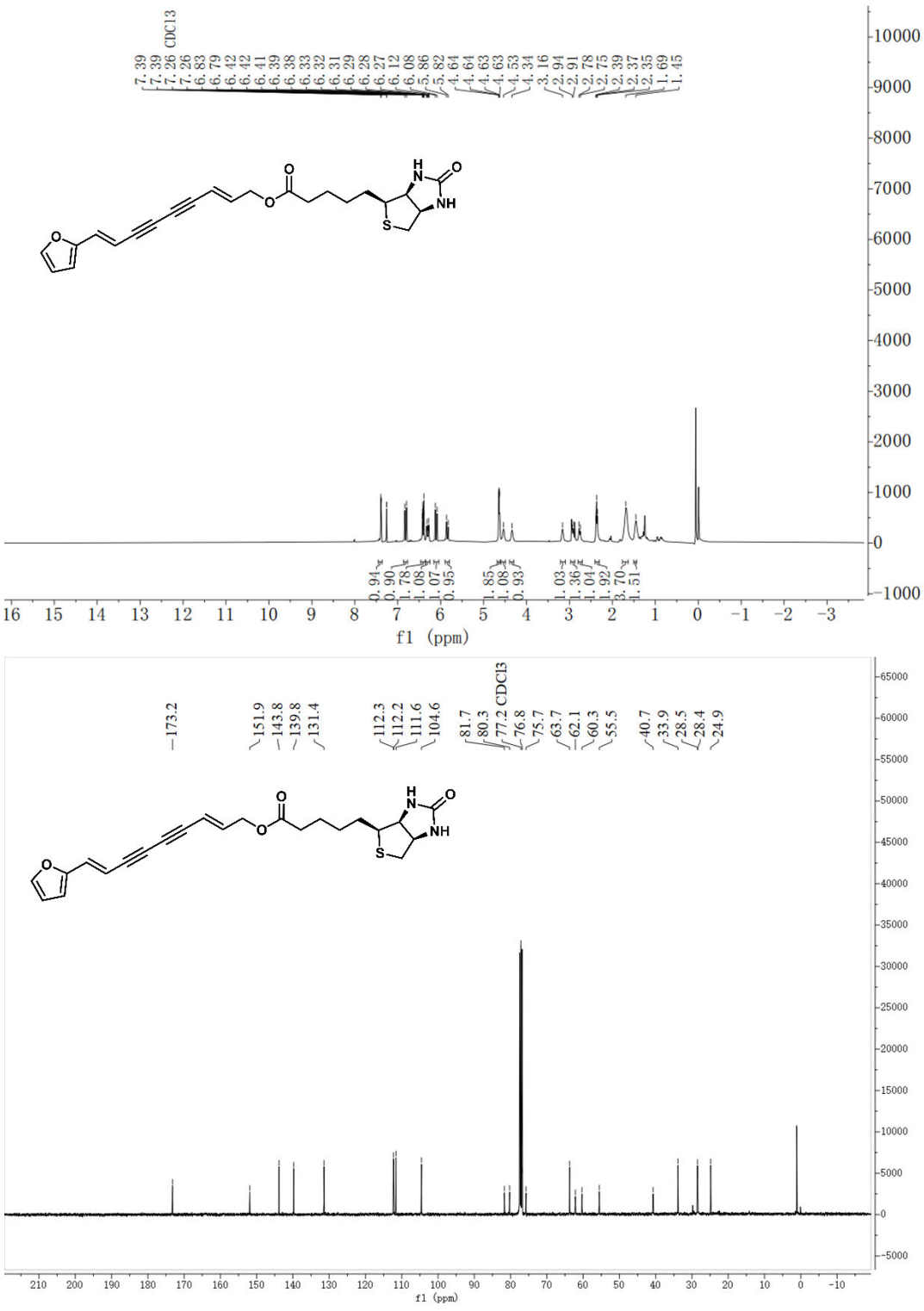

Figure S10. ^{1}H and ^{13}C NMR spectra of ATD-biotin in chloroform-*d*.

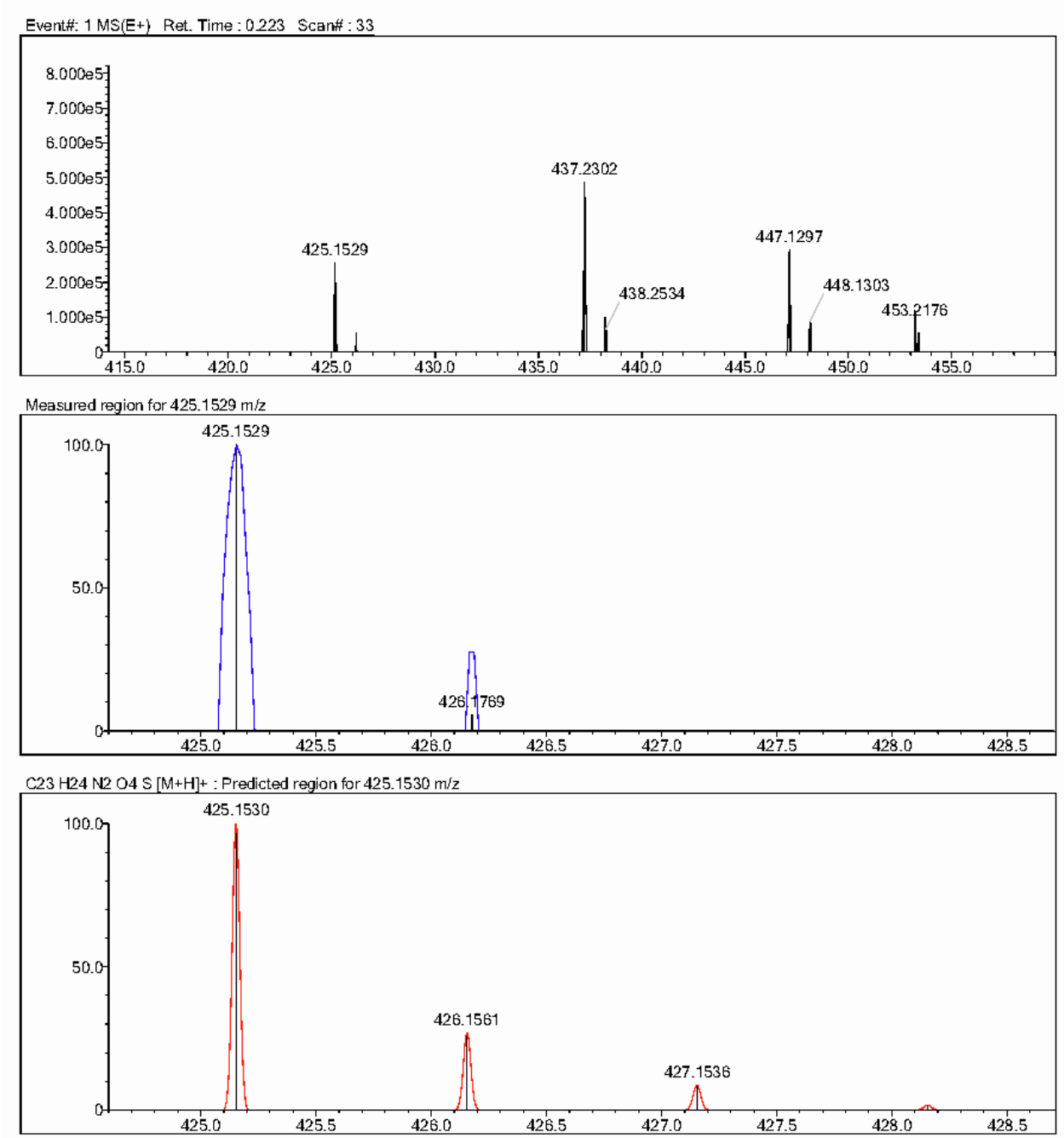

Formula (M)	Ion	Meas. m/z	Pred. m/z	Df. (mDa)	Df.(ppm)	DBE
C23 H24 N2 O4 S	$[M+H]^+$	425.1529	425.1530	-0.1	-0.24	13.0

Figure S11. HRMS spectrum of ATD-biotin.

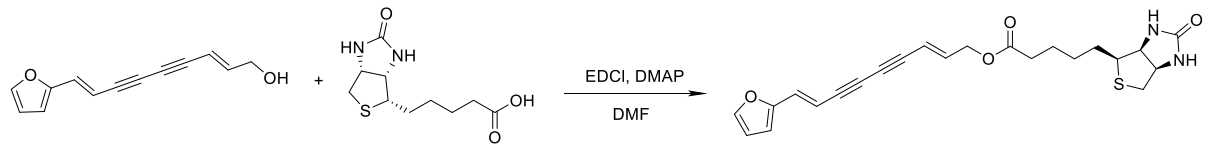

Figure S12. Synthesis of ATD-biotin.

D-Biotin (122.4 mg, 0.5 mmol), DMAP (63.7 mg, 0.5 mmol), and EDCI (75.7 mg, 0.4 mmol) were dissolved in DMF (8.0 mL). The mixture was stirred at room temperature for 30 min. Atractylodinol (73.2 mg, 0.4 mmol) was dissolved in DMF (2.0 mL), then added to the mixture. The reaction mixture was stirred at room temperature for 18 hours under N_2 environment and protected from light. And then water (20.0 mL) was added and the mixture was extracted with CH_2Cl_2 (3×). The combined organic layer was washed with saturated NH_4Cl (aq), water, and saturated NaCl (aq) in turn, dried over Na_2SO_4, and concentrated under reduced pressure. The residue was purified by silica gel chromatography, eluting with a gradient of 0 to 100% MeOH in CH_2Cl_2, to provide ATD-biotin (26.5 mg,16.9 % yield) as a brown solid.

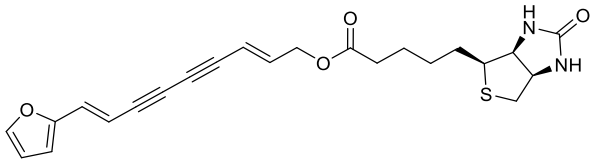

Figure S13. ATD-biotin chemical structure.

ATD-biotin: brown solid, 38 %.^{1}H NMR (400 MHz, Chloroform-*d*) δ_H 7.39 (br s, 1H), 6.81 (d, *J* = 16.0 Hz, 1H), 6.44 − 6.37 (m, 2H), 6.30 (dt, *J* = 16.0, 5.7 Hz, 1H), 6.10 (d, *J* = 16.0 Hz, 1H), 5.84 (d, *J* = 16.0 Hz, 1H), 4.67 − 4.60 (m, 2H), 4.53 (br s, 1H), 4.34 (br s, 1H), 3.16 (br s, 1H), 2.96 − 2.85 (m, 2H), 2.71 − 2.79 (m, 1H), 2.37 (t, *J* = 7.3 Hz, 2H), 1.77 − 1.59 (m, 4H), 1.42 − 1.48 (m, 2H).^{13}C NMR (100 MHz, Chloroform-*d*) δ_C 24.9, 28.4, 28.5, 33.9, 40.7, 55.5, 60.3, 62.1, 63.7, 75.7, 76.8, 80.3, 81.7, 104.6, 111.6, 112.2, 112.3, 131.4, 139.8, 143.8, 151.9, 173.2. HRMS (ESI): calcd for $C_{23}H_{25}N_2O_4S$ $[M+H]^+$ 425.1530, found 425.1529.

Table S1. Acute toxicity in mice by up-and-down method.

Group	Dose (mg/kg)	Log Dose	Mortality rates (%)	Deaths (n)	Survivals (n)
1	175	2.2	0	0	2
2	550	2.7	0	0	2
3	1750	3.2	0	0	6
4	5000	3.7	100	6	0
Estimated LD_{50} = 3129 mg/kg.					
95% confidence interval = 1750 - 5000 mg/kg.					

Table S2. Organ weights were relative to body weight (percentage body weight). The organ coefficients was calculated as body weight (g) divided by organ weight (g). $n = 8$. Data were presented as the mean ± SEM. $^{\#}P < 0.05$, $^{\#\#}P < 0.01$, $^{\#\#\#}P < 0.001$ compared to the control group. $^{*}P < 0.05$, $^{**}P < 0.01$, $^{***}P < 0.001$ compared to the bleomycin group.

Organs	Control	BLM	ATD (2.5 mg/kg)	ATD (5 mg/kg)	ATD (10 mg/kg)	PFD (300 mg/kg)
Body weight (g)	23.10 ± 1.41	13.41 ± 2.02###	20.55 ±3.07***	21.22 ± 0.70***	22.14 ± 1.27***	20.18 ± 3.65***
Lung (% BW)	0.93 ± 0.01	1.60 ± 0.06##	1.08 ± 0.03*	0.91 ± 0.02***	0.84 ± 0.01***	0.84 ± 0.01*
Heart (% BW)	0.59 ± 0.07	0.60 ± 0.08	0.60 ± 0.03	0.58 ± 0.06	0.57 ± 0.08	0.93 ± 0.01
Liver (% BW)	4.44 ± 0.06	4.14 ± 0.05	4.09 ± 0.05	4.34 ± 0.06	4.15 ± 0.04	4.97 ± 0.05*
Kidney (% BW)	0.62 ± 0.01	0.64 ± 0.04	0.66 ± 0.01	0.68 ± 0.07	0.66 ± 0.06	0.65 ± 0.01
Spleen (% BW)	0.27 ± 0.06	0.28 ± 0.06	0.27 ± 0.05	0.27 ± 0.03	0.25 ± 0.05	0.24 ± 0.06

Table S3. Serum biochemical in mice. $n = 8$. Data were presented as the mean ± SEM. $^{\#}P < 0.05$, $^{\#\#}P < 0.01$, $^{\#\#\#}P < 0.001$ compared to the control group. $*P < 0.05$, $**P < 0.01$, $***P < 0.001$ compared to the bleomycin group.

Blood parameters	Control	BLM	ATD (2.5 mg/kg)	ATD (5 mg/kg)	ATD (10 mg/kg)	PFD (300 mg/kg)
ALP (U/L)	116.00 ± 3.65	134.00 ± 6.56	133.60 ± 6.40	128.00 ± 2.31	142.00 ± 5.72	137.20 ± 8.80
ALT (U/L)	30.67 ± 2.67	34.80 ± 2.53	37.20 ± 2.07	37.14 ± 3.87	34.86 ± 3.46	39.00 ± 3.00
AST (U/L)	112.00 ± 8.33	124.00 ± 7.17	121.78 ± 8.14	126.00 ± 7.04	117.71 ± 9.39	106.80 ± 9.11
CREA (μmol/L)	14.00 ± 0.89	17.20 ± 0.85	16.80 ± 1.16	18.22 ± 0.97	18.00 ± 1.37	20.00 ± 1.79$^{\#}$
BUN (mmol/L)	16.91 ± 1.38	17.36 ± 1.00	16.06 ± 0.47	15.03 ± 0.58	17.62 ± 0.89	15.61 ± 0.71
CK (U/L)	1084.67 ± 99.84	1284.00 ± 95.51	1128.00 ± 99.95	1184.00 ± 94.23	1078.29 ± 98.82	1157.60 ± 91.25
CHO (mmol/L)	2.71 ± 0.14	2.44 ± 0.05	2.46 ± 0.09	2.65 ± 0.09	2.74 ± 0.07	2.65 ± 0.06
TG (mmol/L)	0.66 ± 0.07	0.78 ± 0.05	0.56 ± 0.04	0.61 ± 0.08	0.75 ± 0.09	0.79 ± 0.09
LDH (U/L)	575.33 ± 39.52	586.80 ± 53.85	462.00 ± 30.237	456.50 ± 18.09	472.00 ± 33.76	432.67 ± 41.97
GLU (mmol/L)	5.69 ± 0.18	5.87 ± 0.15	5.98 ± 0.14	5.67 ± 0.17	5.94 ± 0.13	6.05 ± 011
TBA (mmol/L)	0.667 ± 0.16	2.17 ± 0.55	2.00 ± 0.50	1.80 ± 0.32	1.38 ± 0.46	1.33 ± 0.67

Table S4. Mass Spectroscopy analysis of proteins bound to ATD-biotin in HFL1.

Protein	Accession no.	Coverage %	Peptides	Molecular mass (kDa)
Vimentin	P08670	71	41	53.6
Keratin, type II cytoskeletal 1	P04264	41	28	66
Tubulin beta chain	P07437	30	11	49.8
Pyruvate kinase PKM	P14618	35	16	57.9
ATP synthase subunit alpha, mitochondrial	P25705-1	28	15	59.7
Perilipin-3	O60664-1	21	7	47
Actin, aortic smooth muscle	P62736	23	8	42
Hornerin	Q86YZ3	12	8	282.2
Isoform 2 of Keratin, type II cytoskeletal 8	P05787-2	13	10	56.6
Histone H4	P62805	50	5	11.4

Table S5. Primer sequences for real-time Q-PCR.

Abbreviations	Gene	Forward Primer	Reverse Primer
COL1A1	Collagen type I alpha 1 chain	GCGAGAGCATGACCGATGGATTC	GCCTTCTTGAGGTTGCCAGTCTG
FN1	Fibronectin 1	ATGCAACGATCAGGACACAAGGAC	TGCCTCTCACACTTCCACTCTCC
ACTA2	Actin alpha 2, smooth muscle	CTCTGGACGCACAACTGGCATC	CACGCTCAGCAGTAGTAACGAAGG
VIM	Vimentin	CCTTCGTGAATACCAAGACCTGCTC	AATCCTGCTCTCCTCGCCTTCC
TGFBR1	Transforming growth factor beta receptor 1	CTCTTCAAAAACTGGGTCTGTG	CATCAACATGAGTGAGATGCAG
GAPDH	Glyceraldehyde-3-phosphate dehydrogenase	AGAAGGCTGGGGCTCATTTG	AGGGGCCATCCACAGTCTTC

Table S6. Target sequences of shRNAs.

Name	Sequences (5′ to 3′)
h-Vimentin shRNA#1	5′-GCTAACTACCAAGACACTATT-3′
h-Vimentin shRNA#2	5′-CTCTGGTTGATACCCACTCAA-3′
h-Vimentin shRNA#3	5′-GCAGGATGAGATTCAGAATAT-3′
h-Vimentin shRNA#4	5′-CGCCATCAACACCGAGTTCAA-3′

Table S7. Antibodies used for Western blotting and immunofluorescence assay.

Antibody	Species	Catalog Number	Supplier
Vimentin	Rabbit	10366-1-AP	Proteintech
Fibronectin	Rabbit	15613-1-AP	Proteintech
Collagen Type I	Mouse	66761-1-Ig	Proteintech
E-cadherin	Rabbit	20874-1-AP	Proteintech
alpha smooth muscle Actin	Mouse	ab7817	Abcam
TGFβ Receptor I	Mouse	sc-518018	Santa
TGFβ Receptor II	Mouse	sc-17792	Santa
Phospho-Smad2 (Ser255)	Rabbit	ab188334	Abcam
Phospho-Smad2 (Ser465/Ser467)	Rabbit	18338	Cell Signaling Technologies
Smad2	Rabbit	ab40855	Abcam
Phospho-Smad3 (Ser465/Ser467)	Rabbit	Ab52903	Abcam
Phospho-Smad3 (Ser204)	Rabbit	Ab63402	Cell Signaling Technologies
Smad3	Rabbit	ab40854	Abcam
Smad7	Mouse	sc-365846	Santa
Smad4	Mouse	sc-7966	Santa
TGFβ 1	Rabbit	ab215715	Abcam
Erk1/2	Rabbit	4695	Cell Signaling Technologies
Phospho-Erk1/2	Rabbit	4370	Cell Signaling Technologies
JNK	Rabbit	9252	Cell Signaling Technologies
phospho-JNK	Rabbit	9255	Cell Signaling Technologies
p38	Rabbit	8690	Cell Signaling Technologies
Phospho-p38	Rabbit	4511	Cell Signaling Technologies
Phospho-Vimentin (Ser39)	Rabbit	13614	Cell Signaling Technologies
Phospho-Vimentin (Ser56)	Rabbit	ab217673	Abcam
Phospho-Vimentin (Ser83)	Rabbit	3878	Cell Signaling Technologies